

# 1. Synthesis and research of carbon materials with controlled porosity

## Oglekļa materiālu ar kontrolētu porainību sintēze un izpēte

**Galina Dobele, Aleksandrs Volperts, Lilija Jašina, Aivars Žūriņš**

Latvian State Institute of Wood Chemistry  
Dzērbenes iela 27, Rīga, LV-1006, Latvia  
E-mail: gdobele@edi.lv

### Contents

1. Synthesis and research of carbon materials with controlled porosity . . . . .	9
1.1. Introduction . . . . .	10
1.2. Literature review . . . . .	10
1.2.1. Thermochemical activation . . . . .	10
1.2.2. Hydroxides and salts of alkali metals . . . . .	10
1.2.3. Description of pores. . . . .	11
1.2.4. Development of surface structure of biomass-derived carbon materials. . . . .	11
1.2.5. Carbon materials for electrochemical capacitor electrodes . . . . .	12
1.3. Materials and methods . . . . .	14
1.3.1. Precursor carbonization, activation and demineralization. . . . .	14
1.3.2. Supercapacitor electrodes and testing . . . . .	15
1.3.3. AC testing methods . . . . .	15
1.4. Results. . . . .	16
1.4.1. AC structural properties . . . . .	16
1.4.2. Relationship between AC properties and electrochemical characteristics of SC with inorganic electrolyte. . . . .	17
1.5. Conclusions . . . . .	22
1.6. References . . . . .	22
1.7. Kopsavilkums . . . . .	24

### 1.1. Introduction

The application of activated carbon (AC) and its various modifications is of a significant scientific and practical importance, since the use of these materials in various technological areas is on a constant increase – they can be applied for sorption, in rare earth metal membrane separation, metallurgy, electronics, aero- and space technologies, as well as nuclear energy development.

New studies are devoted to the possibilities of AC application, which are being used and developed in the framework of nanotechnologies [1–3]. Specifics of carbon atom electron shell properties place nanoporous carbon materials (NCM) among the most promising nanomaterials, which can be used in various areas of electronics and energetics [4], [5]. Currently, the investments in nanotechnology account for approximately 9 billion dollars

annually, one third of studies being carried out in the USA. Other important investors are the EU and Japan. There are forecasts predicting that in 2017 the number of employees in nanotechnology-based industries could reach 2 million, and the total value of goods produced by nanotechnologies could rise to 1 trillion dollars.

Development of various types of electrochemical devices using NCM is a prerequisite for long-term ecologically friendly technologies, which, in their turn, can provide the development of many technical areas with minimal energy and reagent consumption.

## 1.2. Literature review

### 1.2.1. Thermochemical activation

Treatment of renewable biomass for the production of highly porous carbonaceous materials using chemical activation is of interest worldwide, since these materials can be impregnated easily [6]. By altering conditions of chemical activation, it is possible to control total porosity, pore size distribution and properties of surface functional groups.

For the production of AC, the most crucial technical and economic conditions are precursor properties, uniformity, availability and low costs of both raw materials and activator.

Contrary to steam activation chemical process is faster and proceeds at lower temperatures [1, 7–9]. The main advantage of thermochemical activation is ability to synthesize AC with higher specific surface, which reaches theoretical limits (more than 3000 m<sup>2</sup>/g according to BET theory) [10, 11]. Usually, alkali metals hydroxides and carbonates are used as activation agents (most often those containing Na and K cations), as well as ZnCl<sub>2</sub>, H<sub>3</sub>PO<sub>4</sub>. In some cases, K<sub>2</sub>S, AlCl<sub>3</sub>, FeCl<sub>3</sub>, SnCl<sub>2</sub>, etc. are used.

Activators can be separated into two groups according to the mechanism of their action: acidic-alkali (ZnCl<sub>2</sub>, H<sub>3</sub>PO<sub>4</sub>) and redox (KOH, NaOH, K<sub>2</sub>CO<sub>3</sub>) mechanism. The details of chemical activation agent interaction mechanisms are not completely explored; however, it is known that agents that belong to both groups activate aliphatic compounds transformations, especially scission of aryl-alkyl C-C bonds. Also, they selectively remove oxygen, hydrogen and other heteroatoms with simultaneous carbonization.

### 1.2.2. Hydroxides and salts of alkali metals

Efficiency of metal hydroxides as activators in redox processes for AC synthesis has been proven repeatedly. Alkali activation process comprises four main stages: 1) impregnation or mixing of precursor with alkali (ratio 1–7 g/g), 2) heating up to activation temperature (700–900 °C); 3) isothermal treatment (1–5 hours) at activation temperature; 4) mixture cooling and AC demineralization [12]–[14]. AC forms in the end of stage three.

Hydroxides of alkali metals interact with coals, wood and its components already at room temperature [15]. In the temperature range 600–800 °C, organic material reactions with alkali are much more vigorous.

Thermally initiated reactions with MeOH (where Me = K<sup>+</sup> or Na<sup>+</sup>) lead to three main processes:

1. formation of metal containing surface complexes;
2. their transformation into carbonates and oxides (mostly Me<sub>2</sub>CO<sub>3</sub> and Me<sub>2</sub>O) as a result of the reaction with C atoms at the edges of graphene layers;
3. reduction of Me<sub>2</sub>CO<sub>3</sub> and Me<sub>2</sub>O to metals and their intercalation into interlayer space of crystallites.

Reduction and intercalation of metals are two main factors defining formation of adsorbent nanoporous structure [16]. If the process takes place in the ideal conditions, the type of precursor (biomass, coal, etc.) is of no real importance. The efficiency of porous structure development is directly dependent on the presence of oxygen in the functional groups of carbon material surface [17]. AC characteristics are also significantly influenced by the ratio MeOH/precursor and type of hydroxide. Without alkali agents, it is virtually impossible to obtain highly porous material with developed nanoporous structure [18].

### **1.2.3. Description of the pore structure**

When the wood is activated, it forms AC with wide spectrum of specific surface and pore size distribution, which are governed by the conditions of activation. AC have a multitude of pores and thus large specific surface, volume and, as a result, high sorption ability (1 g of AC can have the specific surface from 500 to 2500 m<sup>2</sup>/g, depending on the method of synthesis).

AC have macro-, meso- and micropores. Depending on sizes of the molecules to be adsorbed on the carbon surface, it is necessary to synthesize AC with various pore size distributions. Classification of pores is based on their linear sizes, namely, width for slit-like pores, or diameter or radius for cylindrical or spherical ones. According to IUPAC, pores are classified, as follows [8], [19], [20]:

- micropores < 2 nm
- mesopores 2–50 nm
- macropores 50–200 nm

The role of macropores in the sorption process is to provide transport pathways for the molecules of the adsorbed substance and to enable them to reach deeper into the sorbent particles. Their surface is not extensive, around 0.5–2 m<sup>2</sup>/g, and the sorption in these pores is the same as in the case of non-porous carbon with the same chemical composition.

Mesopores are being formed at the stage of carbonization, and at the next step – activation. The most important factor in the synthesis of mesoporous materials is precursor structure. Their specific surface is from 10 up to 400 m<sup>2</sup>/g. Mesopores significantly influence sorption of larger molecules [20].

Micropores form, when precursor is activated with oxidation agent or in thermal treatment process in the presence of chemical activator. The main property of micropores is that their size is comparable to the size of adsorbed molecules and adsorption energy in these pores is higher than in macro- and mesopores. Micropores have considerable sorption volumes and play the main role in sorption processes [1]. Term “nanopores” is often used as a synonym for micropores.

Ability of AC to adsorb various molecules is governed by its surface structure, as well as composition of surface functional groups and their composition. The most reaction able are oxygen containing functional groups, such as phenol-, carbonyl-, carboxyl-, ether-, enol- and lacto [1], [8]. For the industrial applications, the brands of AC are described by using specific porosity parameters, adsorption ability and particle sizes. Nowadays, 40% of AC is being produced from wood, 40% – from brown coal or lignite, 10% from peat and around 10% from coconut shells [1].

### **1.2.4. Development of surface structure of biomass-derived carbon materials**

Development of surface structure of the biomass-derived carbon materials takes place at the all stages of their thermal treatment. In the temperature range of 600–1000 °C,

heteroatoms are being removed from precursor, carbon partially transforms into  $sp^2$ -hybridization state and is partially removed in a form of volatile or liquid products. In the bulk form of carbon material solid network, graphene structures consist of flat polynuclear aromatic molecules with two-dimensional distribution of carbon atoms. With the increase of temperature, the parallel graphene layers form clusters, which size and structural distribution degree increase with the increase of treatment temperature [21].

Charcoals have a low porosity and consist of elementary crystallites, which are separated with slit-like pores, however, these pores are filled and blocked with chaotic carbon residue (coke). In the process of activation, the filled pores open up and porosity develops. By varying precursor and activation conditions, it is possible to control total porosity and pore size distribution.

The increase of the temperature intensifies condensation reactions, thereby starting the localization of graphite units and formation graphite-like microcrystalline structure, or, in other words, the coalescence of aromatic layer or “graphene planes”. [21].

Carbon material properties and activation conditions define the size and number of graphene layers, and sizes and orientation of crystallites define material's texture and electric conductivity.

Activated carbon structure consists of flat layered packages formed by condensed hexagonal rings of aromatic carbon. The orientation of separate moieties in microcrystallites is random, and the layers are independently tilted towards one another [22] – this kind of structure is called turbostratic. The average thickness of microcrystallites is 1–1.3 nm, which means that they contain 13–20 condensed hexagonal aromatic ring layers [23]. At the next stage of activation, a part of microcrystalline aromatic rings burns out and slit-like pores form – not only between the borders of crystallites, but also inside their bulk.

Carbon has four allotropic forms – diamond ( $sp^3$  – hybridization), graphite ( $sp^2$  – hybridization), nanotubes ( $sp^2$  – hybridization), carbene ( $sp$  – hybridization) and fullerenes (twisted  $sp^2$  – hybridization). Only two of these forms, namely, diamond and graphite, can be found in nature, others are obtained via synthesis. The multiple properties of carbon are not limited by the variety of its allotropic forms and are governed by a number of its physical properties [24].

Carbonization of carbon materials takes place in the solid state, and crystallite mobility is limited, leading to the formation of rigid amorphous structure containing disordered graphene layers. Further thermal treatment does not lead to graphitization, and these materials are being called non-graphitizable carbon forms.

### **1.2.5. Carbon materials for electrochemical capacitor electrodes**

From the 1980s, highly porous carbon materials are being used not only for sorption technologies, but also for electric energy accumulation and transfer without using electrical power sources, as well as for energy consumption peaks. Electrochemical capacitors with double electric layer or supercapacitors (SC) are among the most important developments in this area, and in these devices AC are used as electrodes [25]–[28]. The concept of double electric layer was developed by Helmholtz [29]. The first double layer capacitors were patented by General Electric in 1957 [30]. Charge accumulation and preservation in electrochemical capacitors take place in double electric layer, which forms on the electrode/electrolyte interface, consequently, the electrode material has to meet a number of requirements, such as low density, electric conductivity, and developed porous structure, which should fit ions and molecules of electrolyte (Fig. 1.1).

During charging, the positive charges gradually accumulate on one plate (positive electrode), while the negative charges accumulate on the other plate (negative electrode). When the external voltage difference is removed, both the positive and negative charges remain at their corresponding electrodes. This way, the capacitor plays a role in separating electrical charges. The voltage difference between the two electrodes is called the cell voltage of the capacitor. If these electrodes are connected by using a conductive wire with or without a load, a discharging process occurs—the positive and negative charges will gradually combine through the wire. Thus, the capacitor plays a role in charge storage and delivery [4], [31].

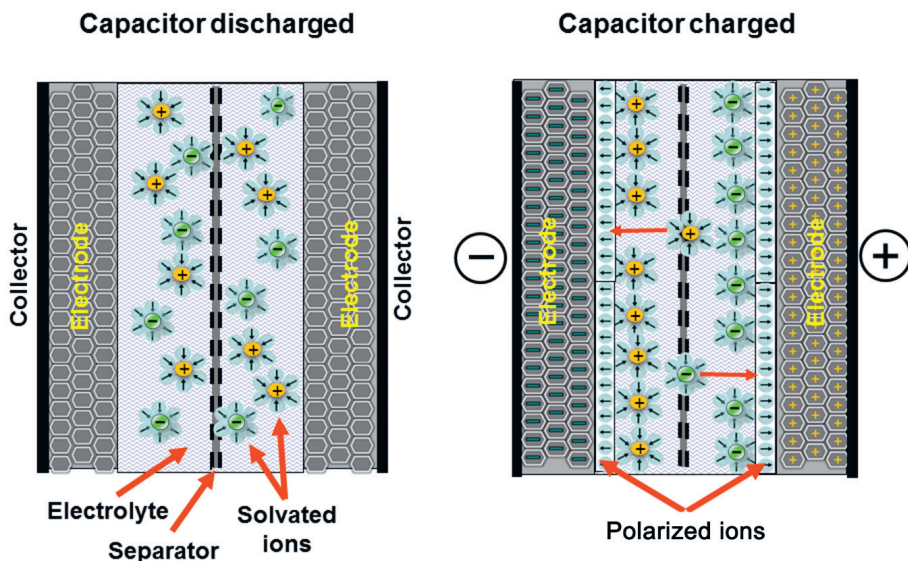


Figure 1.1. Operation principles of supercapacitor

When charged, a capacitor connected in a circuit will act as a voltage source for a short time. Its capacitance ( $C$ ), which is measured in farads (F), is the ratio of electric charge on each electrode ( $Q$ ) to the potential difference between them ( $V$ ), so that [4]:

$$C = Q/V$$

For a typical parallel plate capacitor, capacitance is proportional to the area of each electrode and the permittivity of the dielectric, and inversely proportional to the distance between the electrodes.

Two primary attributes of a capacitor are its energy and power density, both of which can be expressed as a quantity per unit weight (specific energy or power) or per unit volume ( $F/g$  or  $F/mm^3$ ). The energy stored in a capacitor is related to the charge at each interface and the potential difference, and therefore is directly proportional to its capacitance.

Electrochemical double layer capacitors hold the position between batteries, which can accumulate large amounts of energy and conventional capacitors, which can release energy in milliseconds (Fig. 1.2). SC are widely used in automotive production (braking energy recuperation, improvement of engine start up, electrical stabilization), industry (forklifts,

elevators), as well as in customer electronics. SC can provide a higher energy density in comparison with dielectric capacitors, and higher power density than batteries [31], [32]. SC attract interest in various areas, since they are able to release high power in a short period of time – seconds or less. They can be used in cars, trams, buses, construction cranes, lifts and many other appliances. Meeting the demands for worldwide consumption of SC requires both new approaches and electrode material development. The carbon material best suited for this aim has to have low cost, wide nanotexture spectrum and structural variance, as well as high electric conductivity.

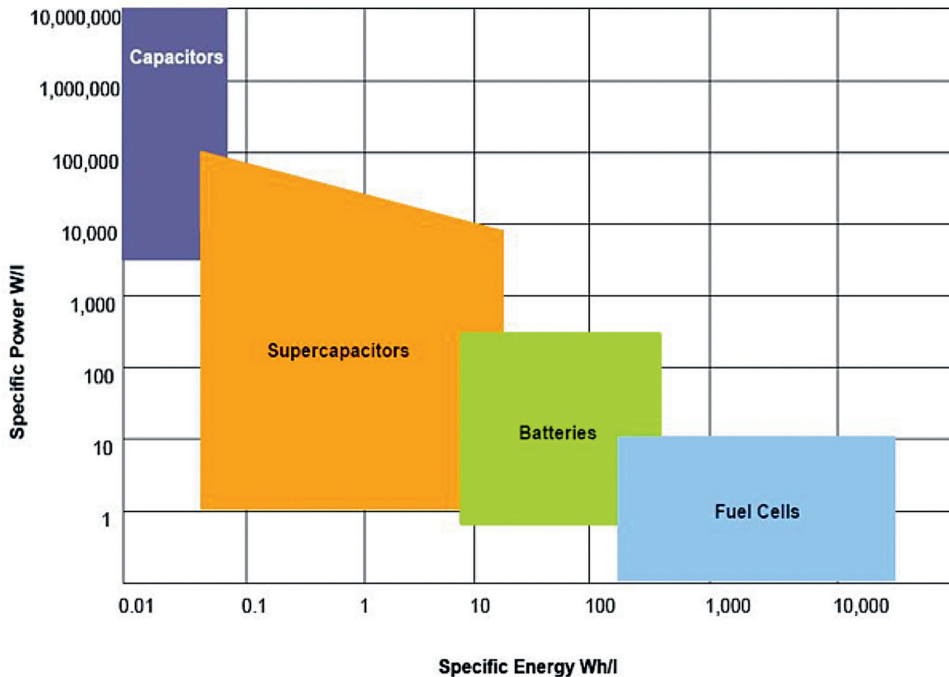


Figure 1.2. Comparison of specific energy and power in dielectric capacitors, SC, accumulators and fuel cells

### 1.3. Materials and methods

#### 1.3.1. Precursor carbonization, activation and demineralization

White alder and birch wood mechanical processing wastes and charcoal (SIA File 2000, Koceni, Latvia) were used as raw materials.

The main stage of AC synthesis from wood and lignocellulosic materials is activation with sodium hydroxide, and the whole process consists of the following steps: 1) Carbonization; 2) Impregnation with alkali; 3) Activation; 4) Demineralization. Two thermal treatment stages are used for the AC synthesis. Carbonization includes heating of precursor up to 300–500 °C and treatment at this temperature for 90–300 min. Activation was performed at 600–800 °C for 60–120 minutes in stream of argon. The schematic representation of AC synthesis is shown in Fig. 1.3.

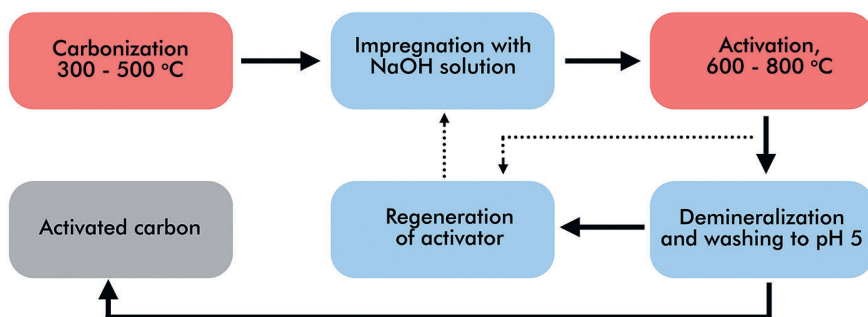


Figure 1.3. AC synthesis on the base of plant biomass

### 1.3.2. Supercapacitor electrodes and testing

AC was mixed with ethanol and then with PTFE water suspension as a binder, which was brought to a pasty condition and then calendared in rollers. Then the electrodes were dried and impregnated with 4.9 M sulfuric acid under vacuum. Porous polypropylene membrane was used as a separator, and 200  $\mu\text{m}$  thermos-expanded graphite foil served as a substrate-current collector. Thus, the mass of the cell includes all of the components mentioned above. Thickness of assembled electrode was 400  $\mu\text{m}$  ( $\pm 10\%$ ), active area of electrodes was 4.15  $\text{cm}^2$ , and areal density was 19–24  $\text{mg}/\text{cm}^2$ . The electrode thickness was chosen as the most important parameter.

SC cell was pressed at 1 MPa between gold plates connected to potentiostat Elins 30-S. Contact resistance between gold plates and SC cell, as well as resistance of wiring was less than 2% of SC intrinsic resistance, and their input was not taken into account for further calculations.

Carbons were tested by cyclic voltammetry. Each SC cell was first cycled in the 0–1000 mV range at 20 mV/s rate until stable voltammograms were observed. Then cells were charged and discharged in the galvanostatic mode with the aim to reach discharge times of 10 and 200 s. The former is related to breaking energy recuperation and the latter to situations, where capacity is not governed by this relatively small current and can be used to assess SC maximum capacitance. Intrinsic resistance was determined from the potential drop on current peak at the initiation of the discharge. To determine power density, SC cells were charged in a potentiostatic mode at 1 V from 5 min. Then cells were charged and discharged aiming at discharge times of 10 and 200 s.

### 1.3.3. AC testing methods

Laser diffraction was used to control changes of AC particles' sizes during refining process. Specific surface, pore size and volume were calculated by using  $\text{N}_2$  adsorption isotherms applying BET, DR and DFT theories. Raman spectroscopy was used to study structural changes of AC. Elemental composition was determined by using CHNS elemental analysis. Study of volatiles formation in carbonization and activation processes was performed by using TG/MS technique. Thermodynamical interaction (heat evolution) determination of activated carbons surface functional groups with liquids depending on activation condition was performed by using immersion calorimetry. Ash content was determined according STM D2866 standard. Microstructure of obtained AC was studied with electron scanning microscopy.

## 1.4. Structural and electrochemical properties of activated carbons

The aim of this study was the elucidation of the dependence of porous structure of alkali activated carbons as a function of synthesis' parameters and measurement of the electrochemical characteristics of supercapacitors made applying AC electrodes.

### 1.4.1. AC structural properties

**AC dispersity.** It is known that when AC are used in electrochemical devices, the electric resistance decreases with the decrease of AC particles' size, since it leads to the enhancement of effective surface contact between power source and electrode, as well as the number of contacts among the particles of active material, which results in a better electron percolation in electrode [33], [34].

Besides, it was found that AC particles decrease down to  $\sim 0.6 \mu\text{m}$  positively influences SC capacity, since it provides for a better pore availability and their decreased depth, which significantly improves migration and adsorption of electrolyte ions [34].

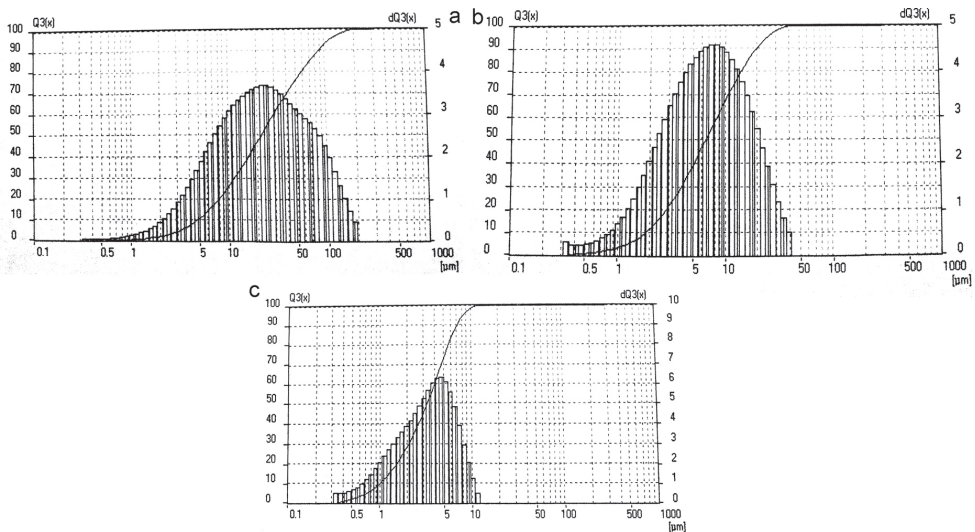
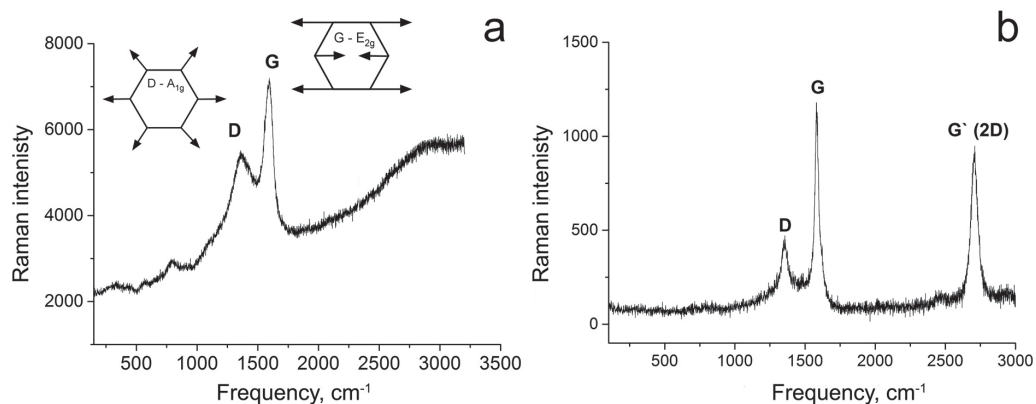


Figure 1.4. AC particle size changes in the process of refining: (a) Retch SM100 knife-type mill; (b) CBM-3H ball mill, 1-hour processing; (c) CBM-3H ball mill, 1-hour processing

To achieve uniform carbonizate particle size, the material first underwent rough treatment in knife-type mill, and then was refined in the ball-type vibrating mill (1 and 2 hours) to achieve particle size in the range of 1–5  $\mu\text{m}$  with a relatively narrow distribution. The changes in material particle size were detected by using laser diffraction (illustration in Fig. 1.4).

It should be noted that SC life cycle is negatively influenced by the particles with sub-micron size [35], thus, the chosen particle size can be asserted as the most beneficial for the study.

**Raman spectroscopy.** The tests of AC structure were performed by using Raman spectroscopy. According to a widespread opinion, solid phase of carbons predominantly consists of polyaromatic graphene clusters (crystallites) [36], [37]. Raman spectra of carbonized wood and AC obtained from carbonized wood at 700 °C in the presence of NaOH are shown in the Fig. 1.5.



**Figure 1.5. Raman spectra of wood carbonizate (a) and AC (Carbonizate-P + NaOH, K = 2, activation temperature 700 °C) (b) (D – amorphous carbon structure; G – graphite structure; G' (or 2D) – two-dimensional carbon structures (graphenes))**

The Raman-active vibration numbering for natural single-crystal graphite exhibits a single Raman peak at around 1580 cm<sup>-1</sup>, called the **G** peak. This peak is associated with the in-plane C–C stretching mode of the *sp*<sub>2</sub> hybridized carbon atoms. For polycrystalline graphite, depending on the size of the crystallites, a second peak at 1350 cm<sup>-1</sup> appears, namely, the disorder or **D** peak. When the degree of material crystallinity decreases carbon phase becomes glassy, both the G and the D peaks broaden (Fig. 1.5 (a)) [38]. Three Raman scattering peaks at around 1364, 1596 and 2325 cm<sup>-1</sup> are observed in the case of AC (Fig. 1.5 (b)). The peak at 1580 cm<sup>-1</sup> (G band) is attributed to an E<sub>2g</sub> mode of graphite and is related to the vibration of *sp*<sub>2</sub> – bonded carbon atoms. For polycrystalline graphite, depending on the size of the crystallites, a second peak at 1350 cm<sup>-1</sup> appears, namely, the disorder or D peak. Decreasing particle size or bending of the lattice fringes may activate this band, and this phenomenon can be observed after activation [38]. Additionally, peak G' (or 2D) ~2500 cm<sup>-1</sup> can be seen for the activated sample (1.5. (b)) – it is characteristic to graphenes and point at the presence of two-dimensional structures.

Raman spectroscopy data allow calculating of crystallites sizes of obtained AC, which is important for stabile operation of electrochemical high capacity devices. As a result of Raman spectra deconvolution and numerical integration, the calculation of average sizes of crystallites for the samples under study ~9.8 nm was implemented, which was beneficial for the electrochemical devices [39].

#### **1.4.2. Relationship between AC properties and electrochemical characteristics of SC with inorganic electrolyte**

In order to evaluate the influence of AC properties on SC characteristics, a number of experiments was performed to assess the most promising conditions of synthesis, which would enable achieving the highest specific capacitance and power of SC. As mentioned before, the most viable raw material for this task is wood carbonizate. It already has been shown [40] that AC obtained from birch or white alder wood have practically identical porous structure properties, and it can be assumed that both wood types are interchangeable within the scope of this work.

Wood-based AC with different NaOH mass ratios to carbonizate (further denoted as K) equal to 3.7 and 1.25 were obtained by using two stage thermochemical synthesis (1 – carbonization at 400 °C, 2 – activation) (Table 1.1, samples T-1 and T-2). Sample T-2 was synthesized from commercial charcoal on the base of white alder (SIA “Fille 2000”) and activated in the same conditions as T-1 without additional carbonization. Comparatively cheap commercial charcoal is considered as a precursor due to three reasons: firstly, it will allow to synthesize AC in one stage, secondly – a local readily available feedstock can be used to synthesize material with a high added value, thirdly – this material has stable properties, and is produced in Latvia in large quantities.

All three samples have high specific surfaces ( $S_{\text{BET}}$  T-1 – 3297 m<sup>2</sup>/g, T-2 – 3304 m<sup>2</sup>/g and T-3 – 1659 m<sup>2</sup>/g), and similar micropore volumes ( $V_{\text{mikro}}$  T-1 – 823 m<sup>3</sup>/g, T-2 – 828 m<sup>3</sup>/g and T-3 – 791 m<sup>3</sup>/g) despite the differences in surface areas. This is an indication of prominent presence of mesoporosity in the structure samples activated at 700 °C and K = 3.7.

All the samples are good candidates for SC or as highly effective sorbents regardless of their differences in porosity. It was found that structural parameters for samples T-1 and T-2 are similar. This is an indication of possibility to use commercial charcoals as a precursor in further experiments.

Samples T-1 and T-2, and commercial AC from various countries were tested as electrodes in SC with H<sub>2</sub>SO<sub>4</sub> electrolyte. For T-1 and T-2, specific capacitances were, respectively, 310 and 318 F/g (Table 1.1).

However, probably due to the high pore volume of synthesized AC, electrodes had low density and, respectively, electrolyte volume was high and inefficient. The high capacity of SC was prominent only based on dry mass calculation, and it was less meaningful, if calculated on the basis of whole cell weight (Table 1.1).

*Table 1.1. Comparison of characteristics of SC with electrodes made from synthesized and commercial AC and carbon fiber cloth (2M H<sub>2</sub>SO<sub>4</sub> electrolyte)*

Sample	Specific capacitance F/g (at 0.3 A/g)	Specific resistance, Ohm/cm	Pore volume (width < 10 nm), mm <sup>3</sup> /g	Electrolyte volume, mm <sup>3</sup> /g	Cell specific power, Wh/kg
<b>T-1 (700 °C, K = 3.7)</b>	<b>310</b>	<b>4.5</b>	1550	2311	<b>2.16</b>
<b>T-2 (700 °C, K = 3.7)</b>	318	<b>4.3</b>	1290	2202	<b>2.23</b>
<b>T-3 (600 °C, K = 1.25)</b>	<b>390</b>	<b>4.6</b>	799	1401	<b>3.06</b>
YP-50F Kuraray (Japan)	182	4	800	1350	1.81
V2 EnerG2 (USA)	182	4	800	1290	1.85
XH-001W Shanxi Xinhui (China)	254	4.4	1000	1670	2.4
Carbon fabric UVIS- AK – T 0.41 (Russia)	211	7.5	370	1170	2.35
Maxsorb-3 (Japan)	320	–	–	2800	–

To elucidate the dependence of SC properties from AC porosity, the unorthodox approach was taken – AC pore volume reduction at varying temperatures and K-ratio. The results of wood-based AC porous structure tests are presented in Fig. 1.6.

Based on the isotherms of AC synthesized in the temperature range 600–800 °C ( $K = 2$ ) (Fig. 1.6 (a)), it can be concluded that adsorbed gas volume increases in activation temperature range from 600 to 700 °C at  $K = 2$  and isotherms belong to Type I, which indicates that AC are microporous. Isotherm of AC activated at 800 °C is different from those of ACs synthesized at lower temperatures and illustrates the presence of both micro- and mesopores. The same effect is observed in Fig. 1.6 (b), showing isotherms of AC activated at 700 °C with  $K$  values between 1 and 3.7. At  $K = 1$  and 2, isotherms correspond to microporous sorbent (Type I) and with the increase of activator/ carbonizate ratio, both the isotherms and adsorption mechanisms are changed.

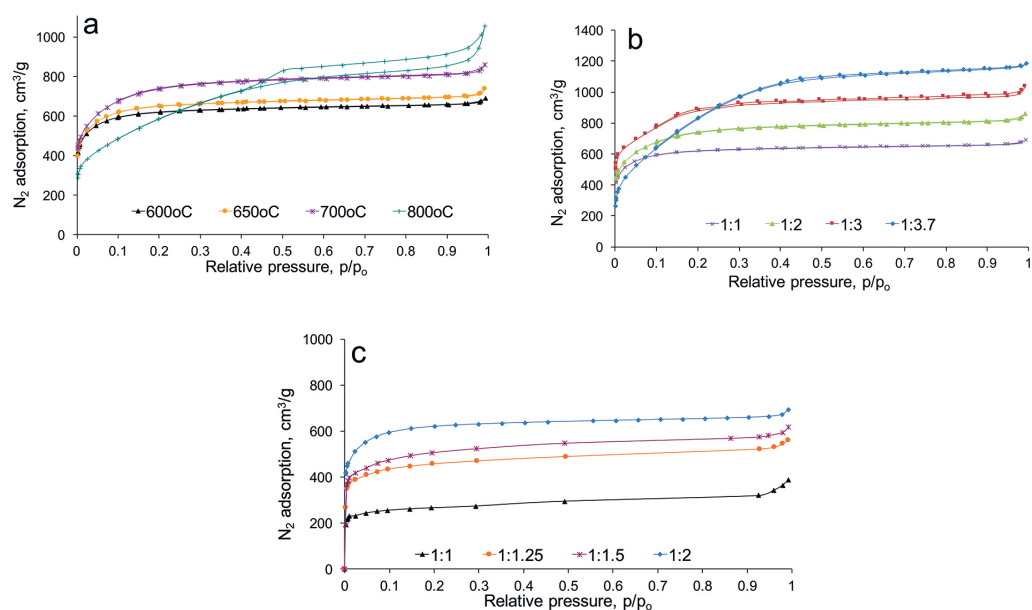


**Figure 1.6.**  $N_2$  adsorption isotherms for AC synthesized in various conditions: (a)  $K = 2$ , activation temperature variation 600–800 °C; (b) activation temperature 700 °C,  $K$  variation 1–3.7; (c) activation temperature 600 °C,  $K$  variation 1–2

At  $K = 3.7$ , the shape of isotherm changes starting at the relative pressure 0.1 and upward, illustrates that pore filling is governed by both volume filling and capillary condensation and that mesopores are present, as well as wider pore size distribution. Isotherms of AC activated at 600 °C and lower  $K$  (Fig. 1.6 (c)) also illustrate that with increasing  $K$  in the range from 1 to 2, the volume of adsorbed nitrogen increases and samples are microporous.

The synthesized AC were used as electrodes in SC cells with sulfuric acid electrolyte. Porous structure and SC characteristics relationships are shown in Fig. 1.7.

The calculations based on data of isotherms show that activator ratio increase ( $K$  varies from 1.5 to 3.7) at 700 °C leads to the development of specific surface ( $S_{\text{BET}}$ ) and total volume ( $V_{\text{total}}$ ), however, micropore volume ( $V_{\text{micro}}$ ) increases until  $K = 2$ , and after that remains practically the same (Fig. 1.7 a). With the increase of pore volume, the amount of adsorbed electrolyte ( $V_{\text{H}_2\text{SO}_4}$ ) increases until  $K = 2.25$ , remains the same until  $K = 3$ , and after that rapidly increases again. With the alteration of activator ration, the specific capacitance of SC changes negligibly. It is the same for all samples in the range of  $K$  from 1.7 to 3.7 – 310 F/g.

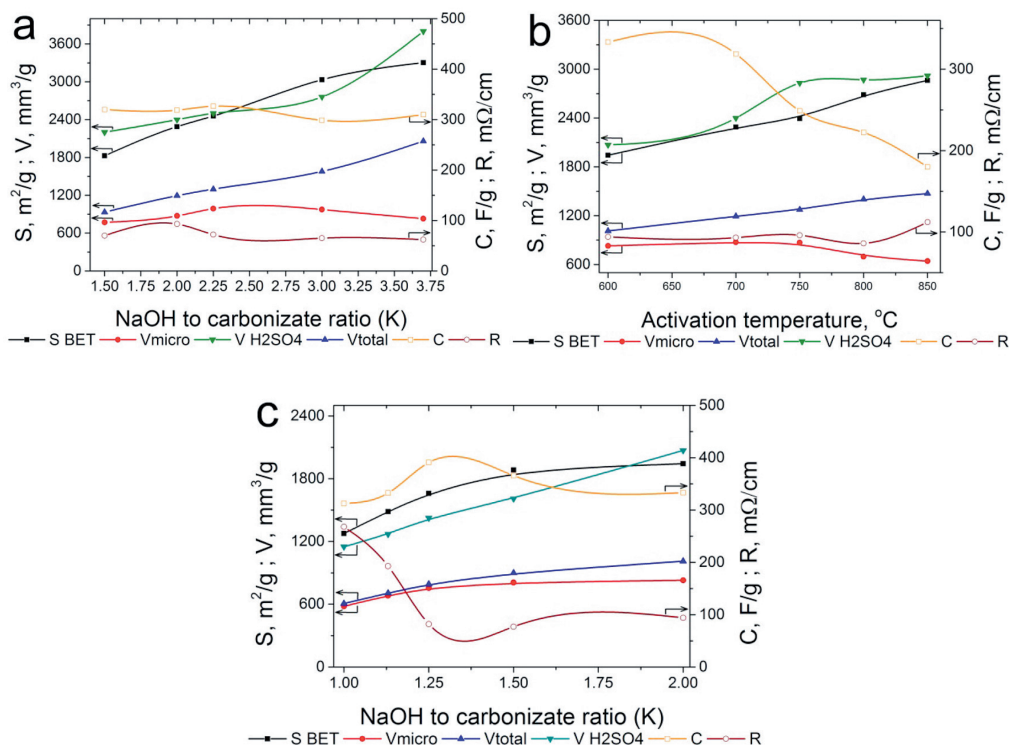


Figure 1.7. Dependence of AC porous structure and SC characteristics from: (a)  $K$  at 700 °C; (b) activation temperature at  $K = 2$ ; (c)  $K$  at 600 °C

$S_{\text{BET}}$ ,  $V_{\text{micro}}$ ,  $V_{\text{total}}$ ,  $V_{\text{H}_2\text{SO}_4}$  – volume of adsorbed electrolyte,  $R$  – resistance and  $C$  – specific capacitance

The insignificant influence of  $K$  at 700 °C on the capacity (Fig. 1.7 (a)) can be explained by the fact that a minimal pore volume is required for the electrical double layer formation. Probably, there is a factor, which counteracts the positive effect of mesoporosity increment – this observation can be interpreted by the change of oxygen-containing functional groups on the surface. These groups can contribute to SC capacitance due to redox reactions (also called the pseudocapacitance effect) and can also elevate the hydrophilicity of surface pores, where EDL is formed. This parameter will be evaluated and discussed further below.

Another important parameter influencing carbon material properties in the process of synthesis is activation temperature. The characteristics of AC activated at 600–850 °C and  $K = 2$  are presented in Fig. 1.7 (b). With the increasing activation temperature keeping the constant activator ratio, the total pore volume does not change significantly, but the micropore volume reaches its maximum at 700 °C, and after that a negative trend can be observed. The same is true for SC capacity, which practically does not change in 600–700 °C range – it is 330 F/g in case of 600 °C, but it is lowered to 180 F/g in case of 850 °C. This means that, in this case, activation temperature and activator ratio decrease positively influences SC electrochemical characteristics, as well as AC production expenses.

At higher activation temperatures, the total volume of electrolyte in the electrodes increases significantly. At the same time, the intrinsic resistance practically does not change with activation temperature increment in the range from 600 °C to 800 °C (Fig. 1.7 (b)). At the higher activation temperatures, the resistance increases, probably due to the presence of larger pore volumes. Most likely, the capacitance decrement with activation temperature increase can be explained by the decrease of C-O groups content on the carbon surface, a parameter, which influences pseudocapacitance.

Thus, the activation temperature decrement positively influenced specific properties of SC taking into account cell mass. The experimental data for AC synthesized at lower activator to precursor ratios and 600°C are presented in Fig. 1.7 (c). The increase of NaOH ratio from 1 to 2 leads to higher values of total and micropore volumes, and in the  $K$  range 1.5–2 the latter does not change. An increase of porosity entails an increase of adsorbed electrolyte volume. With the elevation of  $K$  from 1 to 1.25, the capacitance of SC increases and its resistance rapidly decreases, reaching maximum and minimum, respectively (Table 1.1, sample T-3). With a further increase of  $K$  from 1.25 to 2, the capacity decreases with practically constant values of electrode resistance.

The alterations in wood activation conditions, specifically, decrease of activation temperature and  $K$ , lead to an increase of specific power capacity up to 30% calculating on elementary cell mass.

The activation temperature or/and activator ratio increment lead to formation of additional pores, which adsorb electrolyte. Probably, pore walls become thinner with the increase of activation temperature, which can negatively influence EDL formation. This assumption was proven by authors of [41], who found that potential distribution in CM has the main influence on the system capacity compared to potential distribution in the aqueous electrolyte. Solid phase contribution into the SC intrinsic resistance for the electrolytes with high and low ionic conductivity is different. For the water-based electrolyte with higher ionic conductivity, its effect is more pronounced than that of the organic electrolyte. The lower cell wall thicknesses can have a negative influence on the solid phase coherency, which, in its turn, leads to increase of ohmic losses due to a diminished contact between carbon particles in the electrodes.

Judging from the dependency of SC characteristics on activation temperature, the increase of adsorbed electrolyte volume is not accompanied with intrinsic resistance decrement and specific capacitance increment. This can be explained by two factors. Firstly, deepening of pores can cause difficulties for ion penetration because of gating and uneven charge distribution inside micropores. Secondly, narrower micropores can have a positive influence on specific capacitance due to distortion of ions' solvation shells inside carbon nanostructure, which leads to a closer approach of the ion center to the electrode surface and results in an improved capacitance.

## 1.5. Conclusions

The principal possibility for obtaining of nanoporous activated carbons from hardwood and charcoal by using thermochemical activation, are studied. This research has resulted in award of one international patent and one patent issued in the Republic of Latvia.

The optimal properties of wood thermochemical activation for activated carbons' porous structure formation and adsorption properties, providing necessary electric double layer formation in supercapacitor electrodes were determined.

The correlation was determined between parameters of activated carbon synthesis, porous structure and properties of supercapacitors with aqueous electrolyte. It was found that in the case of sulfuric acid electrolyte application of activated carbon with pore volume  $790 \text{ m}^3/\text{g}$  and specific surface  $1660 \text{ m}^2/\text{g}$  led to development of supercapacitor with specific capacitance of  $390 \text{ F/g}$  and power  $3.06 \text{ Wh/kg}$ .

## 1.6. References

1. Marsh, H. and Rodriguez-Reinoso, F. (eds.). (2006) *Activated Carbon*. Amsterdam: Elsevier Science.
2. Díaz-Terán, J., Nevskaja, D. M., Fierro, J. L. G., et al. (2003) Study of chemical activation process of a lignocellulosic material with KOH by XPS and XRD. *Microporous Mesoporous Mater.*, 60(1–3), 173–181.
3. Lillo-Ródenas, M. A., Juan-Juan, J., Cazorla-Amorós, D. and Linares-Solano, A. (2004) About reactions occurring during chemical activation with hydroxides. *Carbon N. Y.*, 42(7), 1371–1375.
4. Béguin, F. and Frackowiak, E. (eds.). (2013) *Supercapacitors: materials, systems, and applications*. Zurich: Wiley-VCH.
5. Harper, T. (ed.). (2011) Global Funding of Nanotechnologies & Its Impact. *Cientifica*, London, 8.
6. Schüth, F., Sing, K. S. W. and Weitkamp, J. (eds.). (2002) *Handbook of porous solids*. Zurich: Wiley-VCH.
7. Ioannidou, O. and Zabaniotou, A. (2007) Agricultural residues as precursors for activated carbon production. *A review. Renew. Sustain. Energy Rev.*, 11(9), 1966–2005.
8. Bansal, R. C. and Goyal, M. (eds.). (2005) *Activated carbon adsorption*. Taylor & Francis.
9. Микова, Н. М., Иванов, И. П., Парфёнов, В. А et al. (2011) Влияние условий термической и химической модификации на свойства углеродных материалов, получаемых из древесины берёзы. *Журнал Сибирского федерального университета. Серия: Химия*, 4, 356–368.
10. Lillo-Ródenas, M. A., Marco-Lozar, J. P., Cazorla-Amorós, D. and Linares-Solano, A. (2007) Activated carbons prepared by pyrolysis of mixtures of carbon precursor/alkaline hydroxide. *J. Anal. Appl. Pyrolysis*, 80(1), 166–174.
11. Tamarkina, Y. V., Shendrik, T. G., Kucherenko, V. A. and Khabarova, T. V. (2015) Conversion of Alexandriya brown coal into microporous carbons under alkali activation. *Chemistry (Easton)*, 5(1), 24–36.
12. Béguin, F. and Elzbieta, F. (eds.). (2010) *Carbons for electrochemical energy storage and conversion systems*. Boca Raton: CRC Press.
13. Torné-Fernández, V., Mateo-Sanz, J. M., Montané, D. and Fierro, V. (2009) Statistical Optimization of the Synthesis of Highly Microporous Carbons by Chemical Activation of Kraft Lignin with NaOH. *J. Chem. Eng. Data*, 54(8), 2216–2221.
14. Babel, K. and Jurewicz, K. (2004) KOH activated carbon fabrics as supercapacitor material. *J. Phys. Chem. Solids*, 65(2–3), 275–280.

15. Camier, R. and Siemon, S. (1978) Colloidal structure of Victorian brown coals. 1. Alkaline digestion of brown coal. *Fuel*, 57(2), 85–88.
16. McKee, D. W. (1983) Mechanisms of the alkali metal catalysed gasification of carbon. *Fuel*, 62(2), 170–175.
17. Eletsksii, P. M., Yakovlev, V. A., Fenelonov, V. B. and Parmon, V. N. (2008) Texture and adsorptive properties of microporous amorphous carbon materials prepared by the chemical activation of carbonized high-ash biomass. *Kinet. Catal.*, 49(5), 708–719.
18. Тамаркина, Ю. В., Цыба, Н. Н., Кучеренко, В. А and Шендрик, Т. Г. (2013) Получение пористых материалов щелочной активацией ископаемых углей разной степени метаморфизма. *Вопросы химии и химической технологии*, 3, 132–137.
19. Rouquerol, F., Rouquerol, J., Sing, K. S. W., et al. (eds.). (2014) *Adsorption by powders and porous solids*. Academic Press.
20. Gregg, S. J. and Sing, K. S. W. (eds.). (1982) *Adsorption, surface area, and porosity*. London: Academic Press.
21. Кузнецов, Б. Н. (1999) Синтез и применение углеродных сорбентов. *Соросовский образовательный журнал*, No.12, 29–34.
22. Когановский, А. М. (ed.). (1983) *Адсорбционная технология очистки сточных вод*. Киев: Наукова думка.
23. Delhaes, P. (ed.). (2011) *Carbon-based solids and materials*. ISTE.
24. Fitzer, E., Kochling, K.-H., Boehm, H. P. and Marsh, H. (1995) Recommended terminology for the description of carbon as a solid (IUPAC Recommendations 1995). *Pure Appl. Chem.*, 67(3), 473–506.
25. Candelaria, S. L., et al. (2012) Nanostructured carbon for energy storage and conversion. *Nano Energy*, 1(2), 195–220.
26. Inagaki, M., Konno, H. and Tanaike, O. (2010) Carbon materials for electrochemical capacitors. *J. Power Sources*, 195(24), 7880–7903.
27. Qiao, W., Yoon, S. and Isao, M. (2006) KOH Activation of Needle Coke to Develop Activated Carbons for High-Performance EDLC. *Energy Fuels*, 20(4), 1680–1684.
28. Zeng, K., Wu, D., Fu, R., et al. (2008) Preparation and electrochemical properties of pitch-based activated carbon aerogels. *Electrochim. Acta*, 53(18), 5711–5715.
29. Helmholtz, H. (1853) Ueber einige Gesetze der Vertheilung elektrischer Ströme in körperlichen Leitern mit Anwendung auf die thierisch-elektrischen Versuche. *Ann. der Phys. und Chemie*, 165(6), 211–233.
30. Becke, H. I. (1954) *Low voltage electrolytic capacitor*, US2800616 A.
31. Yu, A., Chabot, V. and Zhang, J. (eds.). (2013) *Electrochemical supercapacitors for energy storage and delivery: fundamentals and applications*. CRC Press.
32. Conway, B. E. (ed.). (1999) *Electrochemical Supercapacitors Scientific Fundamentals and Technological Applications*. Kluwer Acad., Plenum., NY, p. 736.
33. Pandolfo, A. G., Wilson, G. J., Huynh, T. D and Hollenkamp, A. F. (2010) The influence of conductive additives and inter-particle voids in carbon EDLC electrodes. *Fuel Cells*, 10(5), 856–864.
34. Portet, C., Yushin, G. and Gogotsi, Y. (2008) Effect of Carbon Particle Size on Electrochemical Performance of EDLC. *J. Electrochem. Soc.*, 155(7), A531.
35. Rennie, A. J. R., Martins, V. L., Smith, R. M. and Hall, P. J. (2016) Influence of Particle Size Distribution on the Performance of Ionic Liquid-based Electrochemical Double Layer Capacitors. *Sci. Rep.*, 6(1), 22062.
36. Shabalina, I. L. (2014) *Ultra-High Temperature Materials I Carbon (Graphene/Graphite) and Refractory Metals*. A Comprehensive Guide and Reference Book.
37. Aliofkhaei, M., Ali, N., William, W. I., et al. (2016) *Graphene science handbook. Fabrication methods*. CRC Press.
38. Lazzarini, A., et al. (2016) A comprehensive approach to investigate the structural and surface properties of activated carbons and related Pd-based catalysts. *Catal. Sci. Technol.*, 6(13), 4910–4922.

39. Cançado, L. G., et al. (2006) General equation for the determination of the crystallite size  $L_a$  of nanographite by Raman spectroscopy. *Appl. Phys. Lett.*, 88(16), 163106.
40. Dobele, G., Vervikishko, D., Volperts, A. and Bogdanovich, N. (2013) Characterization of the pore structure of nanoporous activated carbons produced from wood waste. *Holzforschung*, 67(5), 587–594.
41. Shkolnikov, E. I., Sidorova, E. V., Malakhov, A. O., Volkov, V. V., Julbe, A., and Ayrál, A. (2011) Estimation of pore size distribution in MCM-41-type silica using a simple desorption technique. *Adsorption*, 17(6), 911–918.

## 1.7. Kopsavilkums

Aktivētā oglekļa (AO) un dažādu tā modifikāciju pielietošanas iespējas mūsdienās izraisa ķīmiķu, fiziķu un citu materiālzinātņu nozaru zinātnieku padziļinātu interesi. Mūsdienās oglekļa materiālu (OM) struktūras izpētei ir būtiska zinātniska un praktiska nozīme, jo nemitīgi paplašinās OM izmantošanas iespējas dažādās tehnikas nozarēs, nodrošinot gan retzemju metālu izdališanas membrānu tehnoloģiju, gan radioelektronikas, aviokosmiskās tehnikas un atomenerģētikas attīstības progresu. Jauni pētījumu virzieni ir saistīti ar AO izmantošanu nozarēs, kurās tiek lietotas un attīstītas nanotehnoloģijas. Nanoizmēru struktūras piedod materiāliem noderīgas, bet dažreiz arī unikālas īpašības. Oglekļa atomu elektronu apvalku aizpildīšanas īpatnību dēļ nanoporainie oglekļa materiāli (NOM) ieņem vienu no vadošajām vietām perspektīvo nanomateriālu vidū, piemēram, dažādās stratēģiskās elektronikas un enerģētikas nozarēs. Nanotehnoloģijas izpētes projektu izmaksas mūsdienās visā pasaulē ir vairāk nekā 9 miljardi dolāru gadā. Trešdaļu no visām investīcijām nanotehnoloģijas izpētē veic ASV. Citi galvenie investori nanotehnoloģijas tirgū ir Eiropas Savienība un Japāna. 2017. gadā ar nanotehnoloģijām saistītajās rūpniecības nozarēs strādājošā personāla skaits sasniedza divus miljonus cilvēku, bet ar nanomateriālu tehnoloģijām iegūto preču summārā vērtība rēķināma triljonos dolāru. Dažādas funkcionālas nozīmes elektroķīmisku iekārtu ražošanas attīstība, izmantojot OM, ir priekšnoteikums ilgtspējīgu ekoloģiski tīru tehnoloģiju izstrādei, kas savukārt nodrošina dažādu tehnisku rūpniecības nozaru attīstību ar minimālu enerģijas un reaģentu patēriņu.

Mūsu darbā izpētīta principiāla iespēja un izstrādāti oriģinālas tehnoloģijas pamati nanoporaino aktivēto ogļu iegūšanai termokīmiskās aktivācijas ceļā no lapu koksnes, tās atlikumiem un kokogles.

Noteikti optimālie koksnes termokīmiskās aktivācijas apstākļi aktīvo ogļu porainās struktūras veidošanai un adsorbcijas īpašībām, kas nepieciešami elektriskā dubultslāņa veidošanai superkondensatoru elektrodos. Noteiktas likumsakarības starp aktivēto ogļu iegūšanas apstākļiem, porainas struktūras parametriem un superkondensatora ar ūdens elektrolītu raksturlielumiem. Atrasts, ka sērskābes elektrolīta gadījumā, lietojot ogles ar īpatnējo poru tilpumu  $790 \text{ mm}^3/\text{g}$  un īpatnējo virsmu  $1660 \text{ m}^2/\text{g}$ , superkondensatora kapacitāte bija  $390 \text{ F/g}$  un jauda –  $3,06 \text{ Wh/kg}$ .